

45. MIOCENE STABLE ISOTOPE STRATIGRAPHY, SITE 747, KERGUELEN PLATEAU¹

James D. Wright² and Kenneth G. Miller³

ABSTRACT

We correlated Miocene $\delta^{18}\text{O}$ increases at Ocean Drilling Program Site 747 with $\delta^{18}\text{O}$ increases previously identified at North Atlantic Deep Sea Drilling Project Sites 563 and 608. The $\delta^{18}\text{O}$ increases have been directly tied to the Geomagnetic Polarity Time Scale (GPTS) at Site 563 and 608, and thus our correlations at Site 747 provide a second-order correlation to the GPTS. Comparison of the oxygen isotope record at Site 747 with records at Sites 563 and 608 indicates that three as-yet-undescribed global Miocene $\delta^{18}\text{O}$ increases may be recognized and used to define stable isotope zones. The $\delta^{18}\text{O}$ maxima associated with the bases of Zones Mila, Milb, and Mi7 have magnetochronologic age estimates of 21.8, 18.3, and 8.5 Ma, respectively.

The correlation of a $\delta^{18}\text{O}$ maximum at 70 mbsf at Site 747 to the base of Miocene isotope Zone Mi3 (13.6 Ma) provides a revised interpretation of four middle Miocene normal polarity intervals observed between 77 and 63 mbsf at Hole 747A. Oxygen isotope stratigraphy indicates that the reversed polarity interval at 70 mbsf, initially interpreted as Chronozone C5AAr, should be C5ABr. Instead of a concatenated Chronozone C5AD-C5AC with distinct Chronozones C5AB, C5AA, and C5A (as in the preliminary interpretation), $\delta^{18}\text{O}$ stratigraphy suggests that these normal polarity intervals are Chronozones C5AD, C5AC, and C5AB, whereas Chronozones C5AA-C5A are concatenated. This interpretation is supported by the $\delta^{13}\text{C}$ correlations.

The upper Miocene magnetostratigraphic record at Hole 747A is ambiguous. Two upper Miocene $\delta^{18}\text{O}$ events at Site 747 can be correlated to the oxygen isotope records at Site 563 and 608 using the magnetostratigraphy derived at Hole 747B. Our chronostratigraphic revisions highlight the importance of stable isotope stratigraphy in attaining an integrated stratigraphic framework for the Miocene.

PRINCIPLES OF STABLE ISOTOPE STRATIGRAPHY

Variations in foraminifer $\delta^{18}\text{O}$ records are used widely for Pleistocene stratigraphic correlations and are potentially useful for pre-Pleistocene correlations (Shackleton and Opdyke, 1973; Imbrie et al., 1984; Ruddiman et al., 1986; Williams et al., 1988). Following the pioneering work of Emiliani (1955), Shackleton and Opdyke (1973) designated 22 late Pleistocene $\delta^{18}\text{O}$ cycles as "stages." (In view of changes in stratigraphic nomenclature [Hedberg, 1976; North American Commission on Stratigraphic Nomenclature, 1983], these cycles should now be termed chrons, not stages, when referencing time, or chronozones when referencing sections.) Hays et al. (1976) established that late Pleistocene (0–700 Ka) $\delta^{18}\text{O}$ fluctuations occurred with regular astronomical (Milankovitch) periodicities. Knowing the astronomical forcing allowed Imbrie et al. (1984) to correlate by "tuning" $\delta^{18}\text{O}$ records to Milankovitch periodicities. Imbrie et al. (1984) produced the SPECMAP $\delta^{18}\text{O}$ time scale, which is the standard for late Pleistocene marine correlations. This time scale provides correlations with relative accuracy of 5 k.y. (Imbrie et al., 1984).

Ruddiman et al. (1986), Williams et al. (1988), and Joyce et al. (1990) extended the late Pleistocene "stages" into the early Pleistocene, but their numbering schemes are mutually exclusive (Williams et al., 1988, fig. 15). The possibility of using high-resolution (10^4 – 10^5 yr) oxygen isotope stratigraphy for

pre-Pleistocene correlations was suggested by Ruddiman et al. (1986). Following this lead, Raymo et al. (1988) used high-resolution $\delta^{18}\text{O}$ stratigraphy to correlate upper Pliocene sections from Deep Sea Drilling Project (DSDP) Sites 552 and 607 in the North Atlantic with sections from Ocean Drilling Program (ODP) Site 677 in the eastern equatorial Pacific. Keigwin et al. (1987) similarly noted that high-frequency $\delta^{18}\text{O}$ changes occurred at Site 552 in the late Miocene. Piasis et al. (1985) observed that high-frequency $\delta^{18}\text{O}$ fluctuations occurred in the middle Miocene in the equatorial Pacific at DSDP Site 574. If these high-frequency $\delta^{18}\text{O}$ changes are global, then they have potential for high-resolution stratigraphic correlations.

It has proven difficult to develop a high-resolution (104–105 yr) $\delta^{18}\text{O}$ stratigraphic scheme for the pre-Pliocene because of problems in sampling resolution and stratigraphic correlations. In fact, first-order (m.y. scale) structures are still being identified in the Cenozoic $\delta^{18}\text{O}$ record. Although the general nature of the Cenozoic $\delta^{18}\text{O}$ record was identified by Shackleton and Kennett (1975) and Savin et al. (1975), there are many stable isotope events on the m.y. scale that are only now being recognized. For example, Miller and Fairbanks (1985) and Miller et al. (1989) identified a distinct $\delta^{18}\text{O}$ increase near the Oligocene/Miocene boundary that was previously unknown because of poor sampling in this interval.

Recent studies have shown that stable isotope records can be used to improve pre-Pliocene correlations on the m.y. or finer scale. The key to establishing a stable isotope stratigraphic framework is a firm chronology in the reference section. We have suggested that magnetostratigraphy provides the best chronology for Miocene reference sections, and that stable isotope records must be tied directly to the GPTS (Miller et al., 1985, 1989, 1991a, 1991b). Correlating $\delta^{18}\text{O}$ records from different oceans to polarity patterns establishes synchrony, while it also allows absolute ages to be assigned to identified events.

¹ Wise, S. W., Jr., Schlich, R., et al., 1992. *Proc. ODP, Sci. Results*, 120: College Station, TX (Ocean Drilling Program).

² Lamont-Doherty Geological Observatory and Department of Geological Sciences, Columbia University, Palisades, NY 10964, U.S.A.

³ Department of Geological Sciences, Rutgers University, New Brunswick, NJ 08903, U.S.A., and Lamont-Doherty Geological Observatory, Columbia University, Palisades, NY 10964, U.S.A.

We have used this philosophy to establish formal oxygen isotope zones for the Oligocene-Miocene. Miller et al. (1991b) directly correlated seven Oligocene-Miocene $\delta^{18}\text{O}$ increases to the GPTS on the m.y. scale, and then used them to establish formal isotope zones. They also noted that more events should be found in lower Miocene sections as more detailed records became available.

Knowing the causes of global $\delta^{18}\text{O}$ shifts is not a prerequisite to their use in stratigraphic correlations, but knowing the cause(s) provides a predictive tool for the timing of fluctuations. For example, establishing the Milankovitch forcing mechanism for the late Pleistocene allows "tuning" (i.e., adjusting the correlations of records and their numerical ages) to this known signal (Imbrie et al., 1984). Oligocene to Holocene $\delta^{18}\text{O}$ changes on the m.y. scale may be causally related to eustatic (global sea level) changes. Miller et al. (1991b) proposed that Oligocene to Miocene $\delta^{18}\text{O}$ increases correlate with the second- and third-order sea-level sequence boundaries of Haq et al. (1987). A causal relationship between oxygen isotope increases and sea-level sequence boundaries can facilitate deep-sea and shallow-marine correlations and provide a predictive method to identify isotope events that are not yet known.

Carbon isotopes have not been used as extensively as $\delta^{18}\text{O}$ records for stratigraphic correlation for two reasons:

1. Deep-sea $\delta^{13}\text{C}$ values are nonconservative and represent a composite of several different parameters, including global inventory changes related to the input and output ratios of organic and inorganic carbon, water mass mixing, and deep water aging (Miller and Fairbanks, 1985).

2. Carbon isotopes are used to interpret paleoceanographic changes, making it potentially circular reasoning to correlate with $\delta^{13}\text{C}$ records, and then to interpret paleoceanographic changes using the same records.

Despite these limitations, several Miocene $\delta^{13}\text{C}$ fluctuations have been globally correlated and provide potential for stratigraphic correlations. The most widely known of these is the late Miocene "carbon shift" (Haq et al., 1980), which has been tied not only to the *Amaurolithus datum* (Haq et al., 1980), but also to Chron 6 (Keigwin, 1987). Vincent and Berger (1985) identified a global $\delta^{13}\text{C}$ increase that spanned the early/middle Miocene boundary; Miller and Fairbanks (1985) identified this increase as part of three global Oligocene-Miocene $\delta^{13}\text{C}$ cycles.

At present, Miocene isotope correlations rely heavily on biostratigraphy. Uncertainties in biostratigraphic correlation are typically 0.5–2.0 m.y. in the Miocene (Miller and Kent, 1987), making it difficult to distinguish short-term events (i.e., 10^5 – 10^6 yr duration). Problems arise in many biostratigraphic correlations between the deep-sea and coastal environments because of facies changes and the absence of marker taxa. In addition, comparison of low- and high-latitude isotope records by biostratigraphy alone is difficult because (1) low- and high-latitude biozonations usually are based on different species, and (2) zonal markers may be diachronous across latitude (e.g., Miller et al., 1985). Oxygen isotope stratigraphy provides a means for supplementing biostratigraphy, particularly in correlating high-latitude sections such as Kerguelen Plateau with standard low-latitude stratigraphic schemes.

Stable isotope stratigraphy is not a stratigraphic panacea. As with any stratigraphic scheme that relies on ordinal pattern-matching, stable isotope stratigraphy is based upon matching an unknown record to a known or standard curve. As a result, $\delta^{18}\text{O}$ time series of the unknown section must be fairly complete and represent an interval of time with an

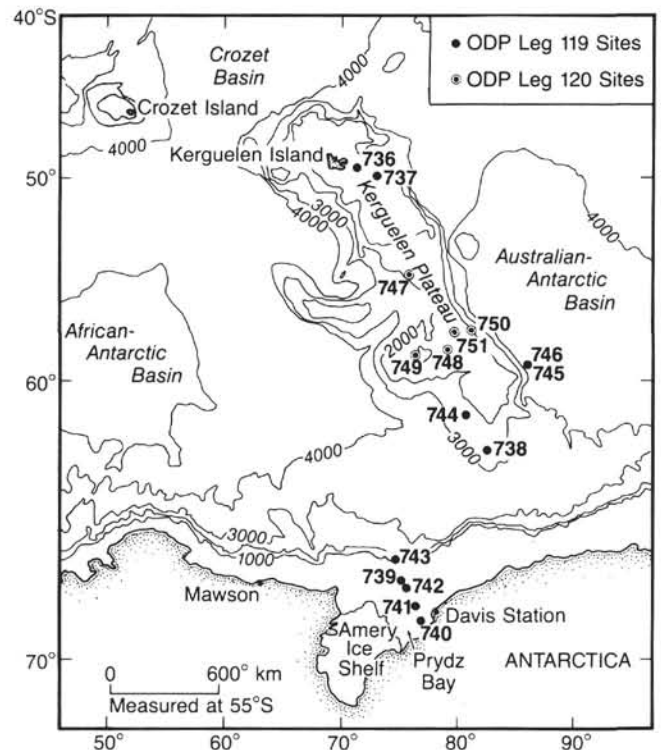


Figure 1. Map showing the location of Site 747 on the Kerguelen Plateau. Also shown are other Leg 120 sites as well as sites from Leg 119.

identifiable event if they are to be stratigraphically useful. Stable isotope records are best used in combination with biostratigraphy or some other stratigraphic framework that is used to establish broad age estimates. Once the general age is known, $\delta^{18}\text{O}$ events can improve stratigraphic correlations to better than 100 k.y., depending on the sampling interval. In this manner, stable isotope stratigraphy works in much the same way as magnetostratigraphy.

Postburial diagenesis can potentially alter the original $\delta^{18}\text{O}$ signal in foraminifer tests, limiting the stratigraphic correlation by stable isotopes (e.g., Killingley, 1983). Diagenetic changes, however, are associated most commonly with burial depths >400 m; sections with burial depths <400 m are usually unaltered (Miller and Curry, 1982; Barrera et al., 1987; Miller et al., 1987). Although the shallow burial depths of the Miocene section at Site 747 (<150 m) do not preclude diagenetic alteration, the lack of optical indications of diagenesis through calcite overgrowths indicates that the $\delta^{18}\text{O}$ recorded at Site 747 was primary.

In this study, we sampled the Miocene section of Site 747 as part of ongoing studies of Miocene stable isotope stratigraphy and paleoceanography. During these investigations it became clear that the oxygen isotope stratigraphy of Site 747 was important for the interpretation of the magnetostratigraphy of this borehole. We present here the stable isotope stratigraphy of the Miocene of Hole 747A and discuss the ramifications of this stratigraphy to the interpretation of the magnetostratigraphy.

LOCATION

Site 747 was drilled in the center of the Kerguelen Plateau ($54^{\circ}48.68'S$, $76^{\circ}47.64'E$) at a water depth of 1695 m (Fig. 1). Site 747 is south of the modern Polar Front and within the flow of the Antarctic Circumpolar Current (ACC). A fairly com-

plete Miocene calcareous ooze section was recovered from Hole 747A in Cores 120-747A-4H to -14H, with an average sedimentation rate for the Miocene of 5 m/m.y. (Schlich, Wise, et al., 1989). Leg 120 was one of the first drilling operations in the Southern Ocean to retrieve a complete middle Miocene section. Previously drilled Southern Ocean DSDP Legs 28 and 35 and ODP Legs 113, 114, and 119 encountered unconformities or siliceous middle Miocene sediments instead of calcareous sediments.

METHODS

Samples were washed with tap water and dried, and *Cibicides* spp. were picked from the >250- μm size fraction. These benthic foraminifers were ultrasonically cleaned for 5 to 10 s and then roasted at 370°C in a vacuum. Oxygen and carbon isotopes were generated at Lamont-Doherty Geological Observatory by a Carousel-48 automatic carbonate preparation device attached to a Finnegan MAT 251 mass spectrometer. The standard deviations, based on 20 NBS-19 measurements made during the analysis of stable isotope data from Site 747, were 0.05‰ and 0.02‰ for $\delta^{18}\text{O}$ and $\delta^{13}\text{C}$, respectively. Replicates of 22 samples indicate that sample variability was 0.10‰ and 0.11‰ for $\delta^{18}\text{O}$ and $\delta^{13}\text{C}$, respectively. These values may overstate the true sample variability because replicates were often chosen for samples that exhibited large isotopic offsets from adjacent sample values. The data are reported in values referenced to PDB (Table 1). The GPTS of Berggren et al. (1985) was used throughout.

DATA

Oxygen Isotopes

The benthic foraminifer $\delta^{18}\text{O}$ record from Site 747 shows patterns similar to those recognized at other sites (Fig. 2). Distinct $\delta^{18}\text{O}$ increases recorded in Miocene benthic foraminifer records can be identified. Oxygen isotope maxima occur at 127.9, 118.4, and 94.1 m below seafloor (mbsf) in the lower Miocene (indicated with arrows in Fig. 2). Oxygen isotope values are fairly constant ($\sim 1.5\text{‰}$) between 107 and 97 mbsf. A pronounced $\delta^{18}\text{O}$ decrease from 1.75‰ to 1.0‰ was recorded over the interval from 94 to 90 mbsf, spanning the lower/middle Miocene boundary. Oxygen isotope values increased between 85 and 84 mbsf, before reaching the lowest $\delta^{18}\text{O}$ value in the Miocene (0.85‰ at 81 mbsf). The middle Miocene section shows the classic "middle Miocene $\delta^{18}\text{O}$ increase" (Shackleton and Kennett, 1975; Savin et al., 1981; Woodruff et al., 1981) in the interval from 79.0 to 62.9 mbsf (Fig. 2). This increase is interrupted from 70 to 67.5 mbsf by a small decrease in $\delta^{18}\text{O}$ values, which lends a steplike appearance to the classic middle Miocene $\delta^{18}\text{O}$ increase. A small (0.5‰) $\delta^{18}\text{O}$ increase was recorded in the upper middle Miocene section at a level of 56.9 mbsf. Upper Miocene $\delta^{18}\text{O}$ values (i.e., above 52 m) continue to increase, punctuated by a $\delta^{18}\text{O}$ increase at 45.4 mbsf.

Carbon Isotopes

Carbon-isotope records show greater variability than the $\delta^{18}\text{O}$ records (Fig. 2). Lower Miocene $\delta^{13}\text{C}$ values record a cycle with minimum values at 117.5 and ~ 103 mbsf, and intervening maximum values of $\sim 1.3\text{‰}$ at 111 mbsf. Carbon-isotope values climb in two steps from 103 mbsf to the highest Miocene $\delta^{13}\text{C}$ values (1.9‰) at 83.4 mbsf. This $\delta^{13}\text{C}$ increase represents the early/middle Miocene increase described by Vincent and Berger (1985). Middle Miocene $\delta^{13}\text{C}$ values were highly variable, with excursions $>0.5\text{‰}$ from 84 to 59 mbsf. Most of the values in this interval were $>1.0\text{‰}$ with maximum $\delta^{13}\text{C}$ values of 1.5‰–1.8‰. Two distinct $\delta^{13}\text{C}$ decreases,

however, were recorded from 70 to 65 mbsf and from 56.9 to 52.5 mbsf (Fig. 2). Upper Miocene $\delta^{13}\text{C}$ values were much lower than those in the middle Miocene and averaged about 1.0‰.

DISCUSSION

The goal of isotope stratigraphy is to improve inter-site correlations. Higher resolution sampling of pre-Pleistocene sections continues to reveal previously unidentified m.y. and k.y. features. Interbasinal correlation of these events requires precise correlations. Magnetostratigraphy provides this precision, although sites within a geographic region may be well correlated with biostratigraphy alone. Unfortunately, not enough magnetostratigraphic records are available for most interbasinal correlations. As a result, correlations must default to biostratigraphy with possibly large uncertainties (Miller and Kent, 1987).

Aliasing the High-frequency Signal

Pisias et al. (1985) noted that a high-frequency signal was embedded in the benthic foraminifer $\delta^{18}\text{O}$ record at Site 574 (central equatorial Pacific) (Fig. 3). Biostratigraphic age models indicate that the high-frequency component appeared to occur in 40-k.y. cycles. Pisias et al. (1985) were careful not to link the $\delta^{18}\text{O}$ cycles changes to orbital forcing without better age control and support from additional records. Regardless of the cause or frequency, undersampling the high frequency signal may alias the record and can yield spurious conclusions (Pisias and Mix, 1988). This is important to consider since our $\delta^{18}\text{O}$ datums are part of a lower frequency cycle ($\sim 1\text{--}2$ m.y.).

We think that aliasing has not compromised our isotope zonations for two reasons: (1) These low-frequency changes (~ 1 m.y.) have been documented in many records of different sampling intervals (see Miller et al., 1991a, for a summary); and, (2) although high-frequency $\delta^{18}\text{O}$ changes are superimposed on the long-term record (Pisias et al., 1985), we can still identify the lower frequency cycles (Fig. 3). Aliasing the high-frequency signal can alter the amplitude of low-frequency cycles. However, the timing of the m.y. cycles can be identified because the high-frequency amplitude is $\sim 0.3\text{‰}$ in comparison to m.y. changes of 0.7‰ to 1.0‰. However, in some cases, aliasing can obscure the m.y. events (e.g., Mi5), making them difficult to recognize because the amplitudes are small (0.5‰–0.6‰) (Fig. 3).

The Million-Year Signals

We have attempted to establish that m.y.-scale variations in the deep-water $\delta^{18}\text{O}$ and $\delta^{13}\text{C}$ records were global by comparing stable isotope and polarity correlations at Site 747 with those at North Atlantic Sites 563 and 608 (Miller et al., 1991b). We can independently verify the paleomagnetic interpretation at Site 747 because we are correlating $\delta^{18}\text{O}$ and $\delta^{13}\text{C}$ records to polarity patterns at more than one site. By correlating isotope events to recognizable polarity patterns at different locations, we establish the synchrony of these events. Uncertainties in the identification of magnetochrons at any site can be clarified by integrating the stable isotope and polarity records from all three sites (see below).

Initial age estimates for the $\delta^{18}\text{O}$ and $\delta^{13}\text{C}$ records at Site 747 were obtained by using the polarity interpretations of Heider et al. (this volume) (Fig. 4). The Miocene $\delta^{18}\text{O}$ record at Site 747 was correlated to standard $\delta^{18}\text{O}$ records at North Atlantic Sites 563 and 608 (Miller et al., 1991a) (Table 2). These North Atlantic locations provide the requisite standards for Miocene isotope zones (Zones Mi2 through Mi6), because they constitute the primary source of first-order correlations of early and middle Miocene $\delta^{18}\text{O}$ events with the GPTS (Miocene isotope Zone Mil

Table 1. Oxygen and carbon isotope data for *Cibicidoides* spp., Hole 747.

Core, section, interval (cm)	Depth (mbsf)	$\delta^{18}\text{O}$	$\delta^{13}\text{C}$
120-747A-			
4H-4, 100-104	33.50	2.296	1.031
4H-4, 100-104	33.50	2.698	0.649
4H-5, 100-104	35.00	2.427	1.344
4H-5, 100-104	35.00	2.525	1.236
4H-6, 100-104	36.50	2.435	1.022
4H-7, 10-14	37.10	2.329	1.176
4H-CC	37.40	2.511	1.284
4H-CC	37.40	2.450	1.299
5H-3, 40-44	40.90	2.509	1.035
5H-3, 105-109	41.55	2.210	0.959
5H-4, 40-44	42.40	2.507	1.106
5H-4, 105-109	43.05	2.356	0.890
5H-5, 40-44	43.90	2.396	1.002
5H-5, 105-109	44.55	2.372	0.872
5H-6, 40-44	45.40	2.532	1.058
5H-6, 105-109	46.05	2.408	1.074
5H-7, 10-14	46.60	2.423	1.063
5H-CC	46.90	2.080	1.031
5H-CC	46.90	2.221	1.055
6H-1, 40-44	47.40	2.310	1.077
6H-1, 105-109	48.05	2.198	0.913
6H-2, 40-44	48.90	2.338	1.089
6H-2, 105-109	49.55	2.191	0.989
6H-3, 40-44	50.40	2.209	0.825
6H-3, 105-109	51.05	2.210	1.004
6H-4, 40-44	51.90	2.207	0.911
6H-4, 105-109	52.55	1.989	0.544
6H-4, 105-109	52.55	2.154	0.675
6H-5, 40-44	53.40	2.249	0.748
6H-5, 105-109	54.05	2.081	1.146
6H-6, 40-44	54.90	2.362	1.473
6H-6, 105-109	55.55	2.184	1.376
6H-7, 10-14	56.10	2.135	1.131
6H-CC	56.40	2.209	0.986
7H-1, 40-44	56.90	2.553	1.435
7H-1, 102-106	57.52	2.039	1.454
7H-2, 40-44	58.40	2.297	1.326
7H-2, 104-108	59.04	2.490	1.453
7H-3, 40-44	59.90	2.449	1.397
7H-3, 100-104	60.50	2.106	1.195
7H-4, 40-44	61.40	2.228	1.093
7H-4, 101-105	62.01	2.064	0.939
7H-5, 40-44	62.90	2.198	1.138
7H-5, 100-104	63.50	2.136	0.930
7H-6, 40-44	64.40	2.354	0.945
7H-6, 100-104	65.00	1.958	0.842
7H-7, 40-44	65.60	2.079	1.285
7H-7, 40-44	65.60	2.001	1.126
7H-CC	65.90	2.218	1.042
8H-1, 40-44	66.40	1.929	1.081
8H-1, 100-104	67.00	1.620	1.009
8H-2, 40-44	67.90	1.732	1.196
8H-2, 100-104	68.50	1.727	1.258
8H-3, 40-44	69.40	1.742	1.495
8H-3, 100-104	70.00	1.733	1.731
8H-3, 100-104	70.00	1.792	1.827
8H-4, 40-44	70.90	1.503	1.231
8H-4, 100-104	71.50	1.402	1.118
8H-4, 100-104	71.50	1.549	1.162
8H-5, 100-104	73.00	1.466	1.502
8H-5, 100-104	73.00	1.692	1.498
8H-6, 40-44	73.90	1.477	1.589
8H-6, 100-104	74.50	1.286	1.623
8H-7, 12-16	75.12	1.166	1.376
9H-2, 40-44	75.90	1.182	1.576
9H-2, 100-104	76.50	1.110	1.478
9H-3, 40-44	77.40	1.132	1.574
9H-3, 100-104	78.00	1.027	1.524
9H-4, 40-44	78.90	0.929	1.357
9H-4, 101-105	79.51	1.301	1.698
9H-4, 101-105	79.51	1.437	1.709
9H-5, 40-44	80.40	1.117	1.482
9H-5, 100-104	81.00	0.846	1.096
9H-6, 40-44	81.90	1.015	1.498
9H-6, 98-102	82.48	1.201	1.674

Table 1 (continued).

Core, section, interval (cm)	Depth (mbsf)	$\delta^{18}\text{O}$	$\delta^{13}\text{C}$
9H-7, 40-44	83.40	1.262	1.890
9H-7, 100-104	84.00	1.479	1.807
9H-7, 100-104	84.00	1.350	1.662
9H-8, 10-14	84.60	1.118	1.646
9H-8, 10-14	84.60	1.149	1.317
9H-8, 40-44	84.75	1.056	1.633
9H-CC	84.90	1.462	1.801
9H-CC	84.90	1.392	1.712
10H-1, 40-44	85.40	1.053	1.522
10H-1, 100-104	86.00	0.972	1.342
10H-2, 40-44	86.90	1.110	1.323
10H-2, 100-104	87.50	1.098	1.486
10H-3, 40-44	88.40	1.159	1.274
10H-3, 100-104	89.00	1.115	1.405
10H-4, 40-44	89.90	1.129	1.216
10H-4, 100-104	90.50	1.087	1.300
10H-5, 100-104	92.00	1.585	1.314
10H-6, 40-44	92.90	1.603	1.339
10H-6, 100-104	93.50	1.359	1.416
10H-6, 100-104	93.50	1.515	1.333
10H-7, 10-14	94.10	1.713	1.382
10H-7, 40-44	94.40	1.436	1.333
11H-1, 40-44	94.90	1.259	1.030
11H-1, 100-104	95.50	1.575	1.186
11H-2, 40-44	96.40	1.649	1.103
11H-2, 102-106	97.02	1.320	0.887
11H-3, 40-44	97.90	1.428	1.037
11H-3, 100-104	98.50	1.464	0.846
11H-4, 40-44	99.40	1.431	0.915
11H-4, 100-104	100.00	1.316	0.795
11H-5, 40-44	100.90	1.391	0.799
11H-5, 101-104	101.51	1.388	0.884
11H-6, 40-44	102.90	1.641	0.830
11H-6, 101-104	103.01	1.371	0.775
11H-7, 10-14	103.60	1.329	0.816
11H-7, 40-44	103.90	1.434	0.955
12H-1, 40-44	104.40	1.447	0.947
12H-1, 100-104	105.00	1.199	0.844
12H-2, 40-44	105.90	1.483	0.922
12H-2, 100-104	106.50	1.500	0.977
12H-3, 40-44	107.40	1.486	1.096
12H-3, 100-104	108.00	1.535	1.018
12H-4, 40-44	108.90	1.375	0.891
12H-4, 100-104	109.50	1.393	0.866
12H-4, 100-104	109.50	1.335	1.044
12H-5, 40-44	110.40	1.673	1.107
12H-5, 100-104	111.00	1.632	1.297
12H-5, 100-104	111.00	1.566	0.931
12H-6, 40-44	111.90	1.599	1.290
12H-6, 100-104	112.50	1.610	0.920
12H-6, 100-104	112.50	1.611	0.927
12H-7, 10-14	113.10	1.421	1.291
12H-7, 10-14	113.10	1.562	0.967
12H-CC	113.40	1.514	1.114
13H-1, 40-44	113.90	1.637	1.145
13H-1, 101-105	114.51	1.352	0.772
13H-2, 40-44	115.40	1.410	0.768
13H-2, 101-105	116.01	1.550	0.864
13H-3, 40-44	116.90	1.534	0.894
13H-3, 101-105	117.51	1.639	0.685
13H-4, 40-44	118.40	1.735	1.113
13H-4, 101-105	119.01	1.519	0.830
13H-4, 101-105	119.01	1.474	0.849
13H-5, 40-44	119.90	1.767	1.023
13H-5, 100-104	120.50	1.517	1.034
13H-5, 100-104	120.50	1.518	0.889
13H-6, 40-44	121.40	1.417	0.810
13H-6, 100-104	122.00	1.380	0.787
13H-7, 10-14	122.60	1.292	0.732
13H-7, 40-44	122.90	1.584	0.829
14H-1, 40-44	123.40	1.633	1.186
14H-1, 102-106	124.02	1.635	1.377
14H-2, 40-44	124.90	1.741	1.186
14H-2, 102-106	125.52	1.642	1.200
14H-3, 40-44	126.40	1.842	1.092
14H-3, 102-106	127.02	1.825	1.004
14H-3, 102-106	127.02	1.478	1.040
14H-4, 40-44	127.90	1.882	1.432

Table 1 (continued).

Core, section, interval (cm)	Depth (mbsf)	$\delta^{18}\text{O}$	$\delta^{13}\text{C}$
14H-4, 102-106	128.52	1.453	1.176
14H-4, 102-106	128.52	1.558	1.192
14H-5, 40-44	129.40	1.687	1.063
14H-5, 101-105	130.01	1.513	1.175
14H-5, 101-105	130.01	1.527	1.253
14H-6, 40-44	130.90	1.530	1.213
14H-6, 101-105	131.51	1.627	1.239
14H-7, 12-16	132.12	1.430	0.865
14H-7, 40-44	132.40	1.331	0.773
15H-1, 40-44	132.90	1.295	0.963
15H-1, 100-104	133.50	1.377	0.963
15H-2, 40-44	134.40	1.358	1.106
15H-2, 100-104	135.00	1.388	1.116
15H-3, 40-44	135.90	1.227	1.183
15H-4, 40-44	137.40	1.389	0.911
15H-5, 40-44	138.90	1.296	0.923
15H-6, 40-44	140.40	1.650	0.912
15H-7, 40-44	141.90	1.449	0.873

is based upon correlations to South Atlantic Site 522; Miller et al., 1991b). Isotope Zones Mi2-Mi6 have been documented in other oceans, but have been directly tied to the GPTS only at Sites 563 and 608. We provide the depth at which each corresponding $\delta^{18}\text{O}$ maximum occurred at Site 747 (Table 2); the maximum was chosen because the isotope zonal boundaries are defined upon the maximum values (Miller et al., 1991b). Ages based upon correlation with Sites 563 and 608 were compared with initial age estimates established from the initial magnetostratigraphic age estimates of Heider et al. (this volume) (Table 2 and Fig. 4).

Implications of Oxygen Isotope Stratigraphy

We have identified Miocene isotope Zones Mi1 through Mi6 at Site 747 following the framework by Miller et al. (1991b) (Fig. 5). At Site 747, $\delta^{18}\text{O}$ maxima at 127.9, 84.9, and 56.9 mbsf are correlated with the Mi1, Mi2, and Mi5 maxima recorded at Sites 563 and 608. The initial age estimates of the Mi1, Mi2, and Mi5 events at Site 747 are 23.7, 16.1, and 11.3 Ma, respectively, and they correspond well with age estimates from Sites 563 and 608 (Table 2 and Fig. 4). This supports the correlation of magnetozones at Site 747 to the GPTS: Chrons C6C, C5C, C5B, and C5r, as determined by Heider et al. (this volume).

There were additional lower Miocene $\delta^{18}\text{O}$ maxima identified at Site 747 at 118.4, 112.5, and 94.1 mbsf (Fig. 2). Two of these maxima were also noted at Sites 563 and 608, but they were not interpreted as global events by Miller et al. (1991b) because of ambiguous polarity records in this interval. For example, the original interpretation of the polarity record at Site 563 by Miller et al. (1985) placed an unconformity at a level of 270 mbsf, separating Chronozones C6n and C5Dr. The isotope data, however, indicate that the polarity change at 270 mbsf at Site 563 is the conformable boundary between Chronozones C5En and C5Dr. Stable isotope evidence indicates that the original identification of Magnetochronozones C6C through C6n at Site 608 by Clement and Robinson (1987) was incorrect (see below).

At Site 747, $\delta^{18}\text{O}$ maxima at 118.1 and 94.1 mbsf have age estimates of 21.8 and 18.1 Ma, respectively, based on correlations with Chronozones C6Ar and C5Dr (Fig. 2). At Site 563, apparently coeval $\delta^{18}\text{O}$ maxima occur in the upper part of Chronozones C6Ar at a level of ~283 mbsf and in Chronozones C5Dr at a level of ~268 mbsf (Fig. 5). The age estimates of these $\delta^{18}\text{O}$ maxima from Site 563 are 21.8 and 18.3 Ma, respectively. Using the revised interpretation of the polarity

record at Site 608 (this study; see also Miller et al., 1991a), $\delta^{18}\text{O}$ maxima at 379 mbsf and 349 mbsf correspond to Chronozones C6Ar and C5Dr and have age estimates of 21.8 and 18.1 Ma, respectively. Based on the documentation of increases in benthic oxygen isotope records at Sites 563, 608, and 747, we formally recognize the maximum $\delta^{18}\text{O}$ values associated with these increases as the base of two zones: Mila and Milb (Appendix).

In the middle Miocene at Site 747, a sequence of four distinct normal polarity intervals from 77 to 62 mbsf was interpreted as Chronozones C5AC/C5AD concatenated (77-72 mbsf), C5AB, C5AA, and C5A (Heider, et al., this volume). Identifying the $\delta^{18}\text{O}$ maximum at 70.0 mbsf at Site 747 as correlative with the $\delta^{18}\text{O}$ increase at the base of Zone Mi3 (13.6 Ma, Table 2 and Fig. 5) yields a different interpretation. At Site 608, the maximum $\delta^{18}\text{O}$ values associated with the base of Zone Mi3 clearly occur within Chronozones C5ABr (Fig. 5) at an estimated age of 13.6 Ma (Table 2). If the level of Zone Mi3 is 70.0 mbsf at Site 747, then the reversed polarity interval at this level must be Chronozones C5ABr and not C5AAr, as interpreted by Heider et al. (this volume). Using this oxygen isotope correlation, Chronozones C5AD, C5AC, and C5AB are distinguished, whereas Chronozones C5AA and C5A are concatenated and are represented by one normal polarity interval between 65 and 61 mbsf. This interpretation is strongly supported by the identification of the $\delta^{18}\text{O}$ increase associated with Zone Mi4 (12.6 Ma) at 64.4 mbsf at Site 747. At Sites 563 and 608, the Mi4 $\delta^{18}\text{O}$ increase occurs within Chronozones C5Ar at an estimated age of 12.6 Ma (Fig. 4). At Site 747, however, the $\delta^{18}\text{O}$ increase falls within a normal interval that must represent the concatenation of Chronozones C5AA and C5A (Fig. 2).

Our interpretations of Chronozones C5-C5A are similar to the reinterpretation of Harwood based on diatoms (pers. comm., 1990). Harwood similarly identifies Chronozones C5B through C5AB from Cores 9 through 8, and places a hiatus during Chron C5AA. Although we cannot confirm a hiatus for this chron, it is consistent with our suggestion of the concatenation of C5AA and C5A.

The initial age estimates of the upper Miocene $\delta^{18}\text{O}$ increases at Site 747 do not agree with the ages estimated by correlation of these increases to Sites 563 and 608. A $\delta^{18}\text{O}$ increase with maximum values at 9.6 Ma was defined as the base of Zone Mi6 (Miller et al., 1991b); we note another $\delta^{18}\text{O}$ increase at 8.5 Ma and use this to recognize Zone Mi7 informally (Appendix). This increase was discussed by Miller et al. (1991b) in records from North Atlantic Sites 563 and 608 and by Wright et al. (1991) for Southern Ocean Site 704. At Site 747, $\delta^{18}\text{O}$ maxima occurred at 9.0 and 8.0 Ma according to the preliminary paleomagnetic age model, whereas Sites 563 and 608 recorded maxima at 9.6 and 8.5 Ma (Table 2). One explanation for the discrepancy is that the long normal of Chronozones C5 is not fully represented at Hole 747A and that the interpretation of Chronozones C4An at 42 mbsf is incorrect. The magnetostratigraphy of this interval appears to be more complete at Hole 747B, and the upper Miocene polarity patterns from Hole 747B better resemble the GPTS than those from Hole 747A (Heider et al., this volume). Applying the magnetostratigraphy of Hole 747B to the oxygen isotope record at Hole 747A, the Mi6 and Mi7 events have estimated ages of 9.3 and 8.4 Ma. These age estimates are in closer agreement with the magnetostratigraphic ages derived from Sites 563 and 608 (9.6 and 8.5 Ma, respectively). It implies that the magnetostratigraphy of the upper Miocene of Hole 747B is correct, and that there is a small offset (<1 m or so) between Holes 747A and 747B.

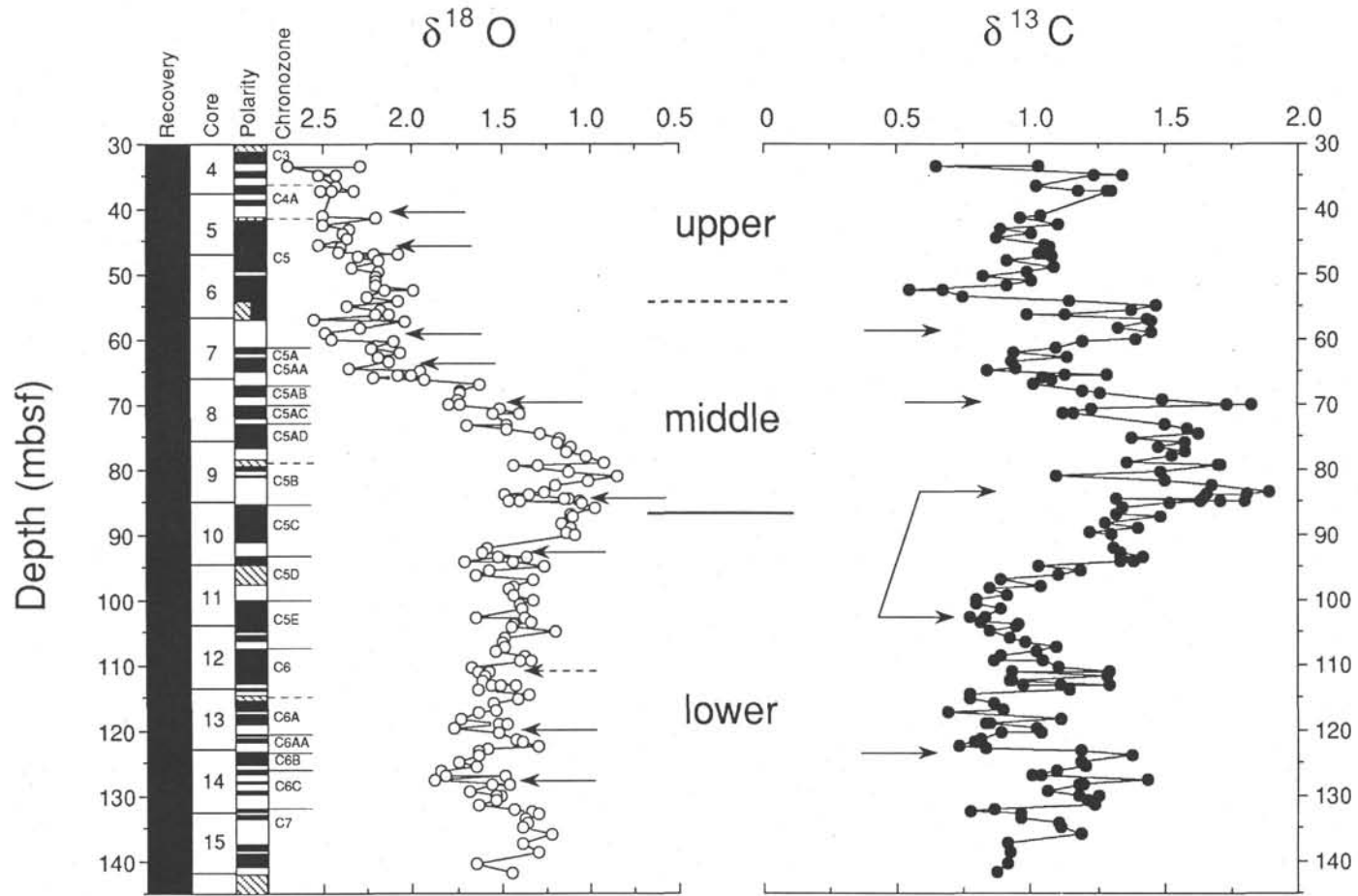


Figure 2. Oxygen and carbon isotope values from Hole 747A plotted vs. depth. Arrows indicate $\delta^{18}\text{O}$ and $\delta^{13}\text{C}$ levels discussed in the text. The magnetic polarity column and the chronozones are reinterpreted from Heider et al. (this volume).

Site 574

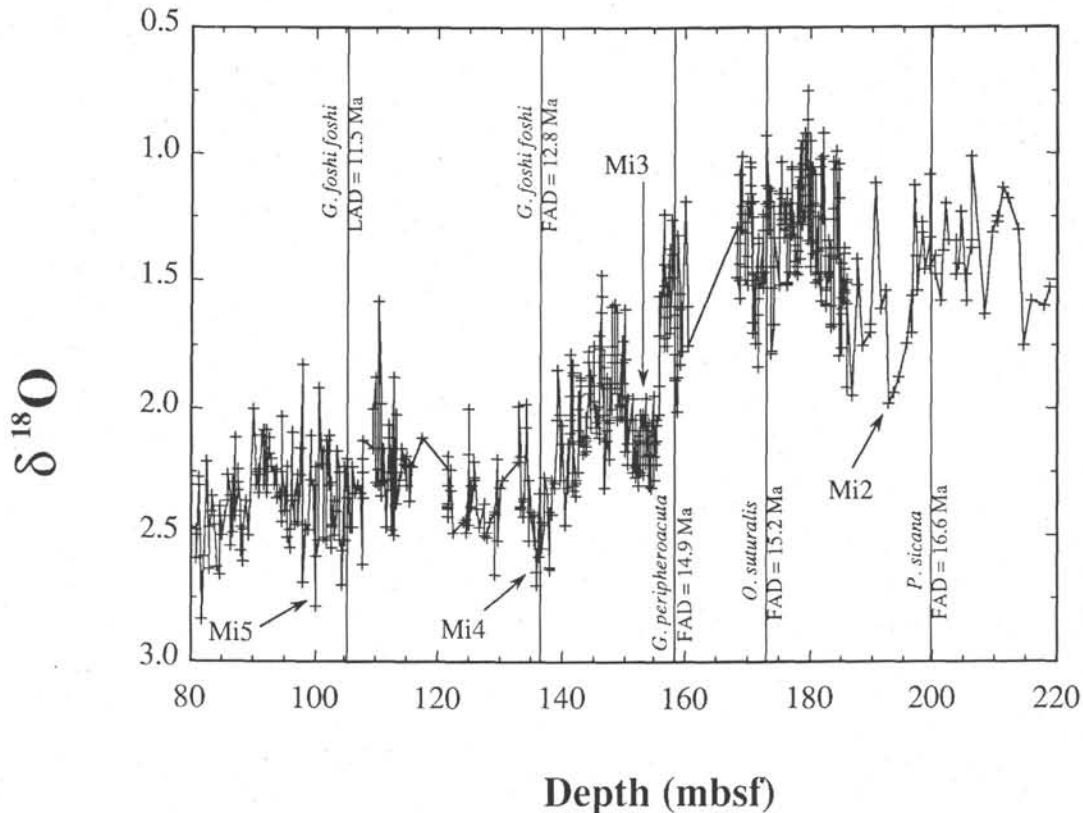


Figure 3. Oxygen isotope record vs. depth from Site 574 (central equatorial Pacific). The isotope data are from Pisias et al. (1985), Shackleton (unpubl. in Woodruff and Savin, 1989), and Woodruff and Savin (in press). The "Mi" maxima are noted on the figure as well as on the planktonic foraminifer FADs and LADs. Age estimates for the biostratigraphic datums are from Berggren et al. (1985).

We revised the initial age estimates by using our oxygen isotope correlations to reinterpret the magnetostratigraphy as discussed above. We then used this revised magnetostratigraphy to estimate revised ages. The revised chronology shows only minor (0.5 m.y. or so) differences from the initial age estimates (Fig. 4). Still, these differences are significant in a detailed interpretation of the stratigraphic correlations of Site 747.

Implications of Carbon-Isotope Records

Although no formal stratigraphic scheme has been based on $\delta^{13}\text{C}$ variations, many studies recognized the global nature of some carbon isotope fluctuations. For example, Vincent and Berger (1985) described a late early Miocene global $\delta^{13}\text{C}$ increase. We established the age of this increase by tying it into the GPTS at Sites 563 and 608 (Fig. 6); from this, an age estimate of 19–16 Ma can be assigned to the increase, based on its position within Chronozones C5E–C5C (top). The $\delta^{13}\text{C}$ increase at Site 747 begins at 103 mbsf in an interval correlated with Chronozones C5En (age estimate = 18.9 Ma) and ends at 84 mbsf (Chronozones C5Br, age estimate = 16.1 Ma) (Figs. 2 and 5). This excellent agreement documents that this $\delta^{13}\text{C}$ increase has not been locally overprinted at Site 747.

A distinct middle Miocene $\delta^{13}\text{C}$ peak can be identified and correlated to the GPTS at Sites 563 and 608. This peak precedes a sharp $\delta^{13}\text{C}$ decrease and occurs within Chronozones C5ABr at Site 608, but it falls within a concatenated Chronozones C5AD–C5AB interval at Site 563. At Site 747, the peak

$\delta^{13}\text{C}$ value is recorded at 70 mbsf. The preliminary magnetostratigraphy indicates that this is Chronozones C5AAr and not C5ABr (Heider et al., this volume). Both oxygen and carbon isotope interpretations, however, indicate that the level of 70 mbsf is best correlated to Chronozones C5ABr and not C5AAr. This implies that the normal polarity intervals from 77 to 63 mbsf should be interpreted as Chronozones C5AD, C5AC, and C5AB, with the last normal representing a concatenation of Chronozones C5AA–C5A.

Another $\delta^{13}\text{C}$ maximum occurred near the top of the middle Miocene within Chronozones C5r (Fig. 6). Age estimates for this maximum are 11.0 at Sites 563 and 608. At Site 747, a $\delta^{13}\text{C}$ increase near the end of the middle Miocene peaked at 56.4 mbsf within a reversed polarity interval recognized as Chronozones C5r. Both the $\delta^{13}\text{C}$ and $\delta^{18}\text{O}$ isotope correlations (Mi5) firmly establish that the position of Chronozones C5r at Site 747 is as in Heider et al. (this volume).

Reinterpretation of Previous Magnetostratigraphic Records

The initial interpretation of the lower Miocene polarity record at Site 608 was complicated by the uncertain identification of Magnetochrons C6A–C6C. A large $\delta^{18}\text{O}$ increase at 411 mbsf at Site 608 was identified as Mi1 (Miller et al., 1991a), and Clement and Robinson (1987) identified this interval of normal polarity as Chronozones C6B. The position of Zone Mi1, however, establishes that this interval must represent Chronozones C6C. The $\delta^{13}\text{C}$ records confirm the misidentification

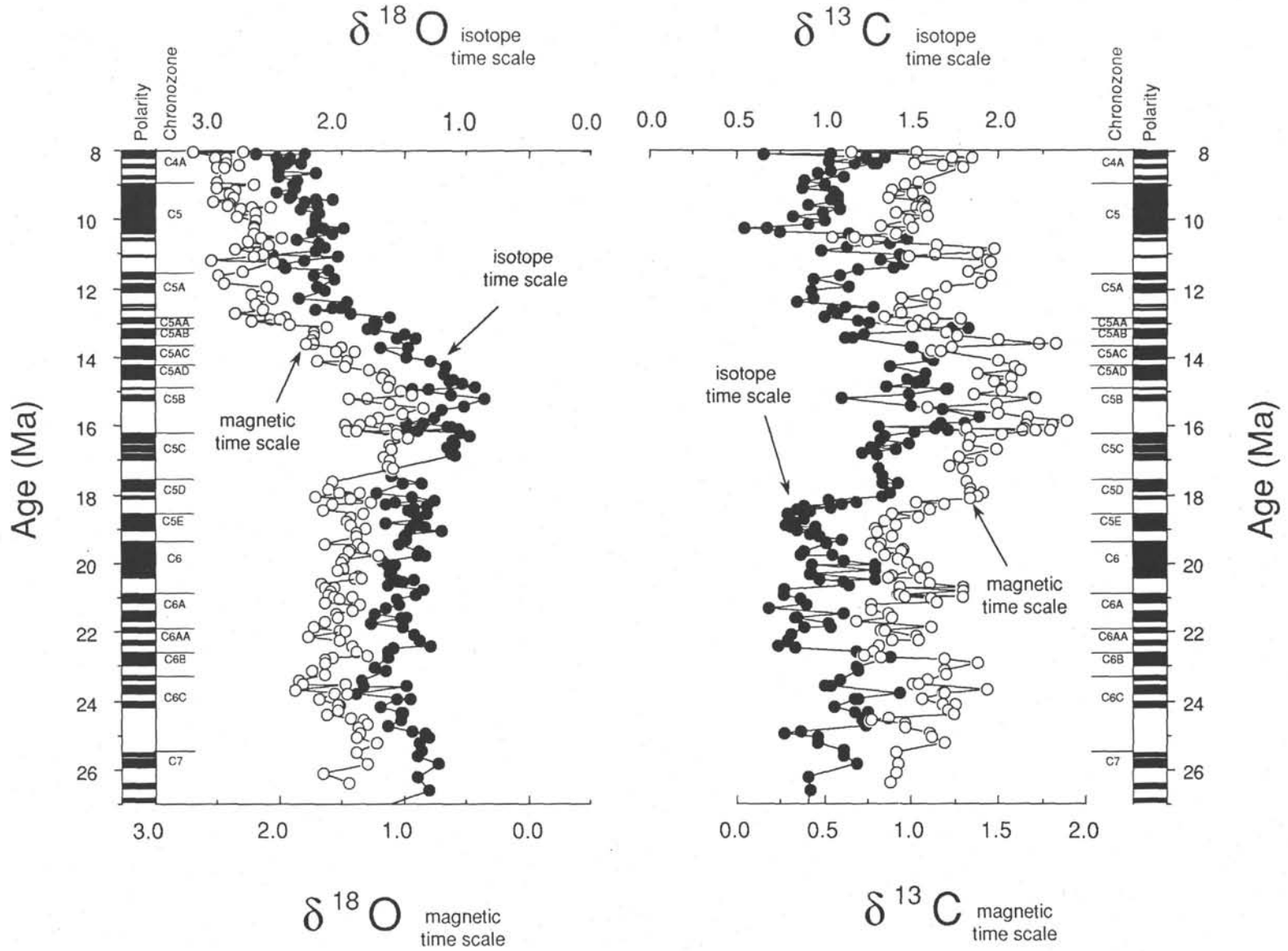


Figure 4. Site 747 oxygen and carbon isotope values plotted vs. age. Two different age models are represented. The line with open circles represents age estimates from the paleomagnetic interpretation of Heider et al. (this volume). The line with closed circles represents age estimates based on Mi-event stratigraphy (see Table 2).

Table 2. $\delta^{18}\text{O}$ event stratigraphy and associated ages.

Event	GPTS correlation	Estimated age ^a (Ma)	Depth at Site 747	Initial age estimate
Mi1b	C6n	(21.7)	117.50	21.4
Mi1c	C5Dn	(18.1)	94.10	17.6
Mi2	C5Br	16.1	84.60	16.1
Mi3	C5ABr	13.6	70.00	13.2
Mi4	C5An	12.6	63.50	12.1
Mi5	C5r	11.3	56.04	11.1
Mi6	C5n	9.6	46.60	9.0
Mi7	base C4n	(8.5)	37.40	8.0

Note: GPTS = Geomagnetic Polarity Time Scale from Berggren et al. (1985). Zone Mi7 is not formally recognized as an isotope chronozone, but it is useful in upper Miocene correlations (Wright et al., 1991).

^aEstimated ages are derived by $\delta^{18}\text{O}$ correlation of Sites 563 and 608 stable isotope events to the GPTS (Miller et al., 1991a) except for the ages indicated in parentheses, which are from Figure 2 (this study).

by establishing the position of the C6AA/C6B boundary. The lower Miocene polarity patterns are clear at Sites 563 and 747. Carbon isotope values decreased across the C6AA/C6B boundary in both records. At Site 608, a $\delta^{13}\text{C}$ decrease in the interval from 395 to 385 mbsf straddles a polarity change at 390 mbsf. Thus, this change must be the C6AA/C6B boundary instead of the C6A/C6AA boundary, as interpreted initially by Clement and Robinson (1986). This reinterpretation of the lower Miocene polarity record is consistent with the $\delta^{18}\text{O}$ and $\delta^{13}\text{C}$ records and it does not violate the biostratigraphic datums at Site 608. We use the revised correlations of the Site 608 record in this study and that of Miller et al. (1991a).

CONCLUSIONS

Oxygen isotope stratigraphy provides a correlation tool independent of biostratigraphy and magnetostratigraphy. Like any ordinal pattern matching technique, stable isotope stratigraphy requires (1) that limits be placed upon the general time interval (e.g., early Miocene), and (2) that the time series be sufficiently long and complete to recognize global patterns. We used our oxygen isotope stratigraphy to evaluate the published preliminary magnetostratigraphy of Hole 747A. The records at Site 747A were correlated to the $\delta^{18}\text{O}$ and $\delta^{13}\text{C}$ records at North Atlantic Sites 563 and 608, which have good magnetostratigraphic control. Hence, we were able to evaluate correlations of Hole 747A to the GPTS in two ways: direct (using the preliminary paleomagnetic record) and indirect (by correlation through Sites 563 and 608). This allowed us to check the magnetostratigraphic interpretations at Site 747.

The complete lower Miocene section at Site 747 provides evidence for two early Miocene $\delta^{18}\text{O}$ isotope increases that were not formally recognized; the maxima associated with these increases are used here to recognize formally the base of two new stable isotope zones (Mila and Milb).

Middle Miocene stable isotope correlations indicate that the preliminary interpretation of Chronozones C5A through C5AD at Hole 747A should be reexamined. A distinct two-tiered step in the "middle Miocene increase" has been identified at Site 747 and in other complete middle Miocene $\delta^{18}\text{O}$ records (e.g., Sites 563 and 608). The base of one of these steps (= base of Zone Mi3, 13.6 Ma) occurred at 70 mbsf at Hole 747A, implying that Chronozones C5ABr, not C5AAr, is at a level of 70 mbsf. This interpretation of the normal polarity events is supported by the presence of a $\delta^{13}\text{C}$ maximum within Chronozones C5ABr. The position of the base of Chronozones

C5 at Hole 747A is well supported by both $\delta^{18}\text{O}$ and $\delta^{13}\text{C}$ records.

We were able to reinterpret the lower Miocene polarity record at Site 608 by integrating the $\delta^{18}\text{O}$, $\delta^{13}\text{C}$, and polarity records from Sites 563, 608, and 747. Both Sites 563 and 747 have clear lower Miocene polarity patterns. The identification of Zone Mi1 at Site 608 is linked to Chron C6C, whereas a distinct $\delta^{13}\text{C}$ decrease correlates with the C6AA/C6B boundary.

ACKNOWLEDGMENTS

We thank E. Thomas, D. Williams, W. Berggren, R. Poore, W. Ruddiman, and D. Kent for reviews, and the shipboard party of Leg 120 for samples from Site 747 for stable isotope analysis. Samples were provided by ODP. This study is part of the Ph.D. thesis of J. D. Wright at Lamont-Doherty Geological Observatory and the Department of Geological Sciences at Columbia University. Research was supported by National Science Foundation Grant No. OCE-88-11834 to K. G. Miller. This is Lamont-Doherty Geological Observatory Contribution No. 4793.

REFERENCES

- Barrera, E., Huber, B. T., Savin, S. M., and Webb, P.-N., 1987. Antarctic marine temperatures: late Campanian through early Paleocene. *Paleoceanography*, 2:21-47.
- Berggren, W. A., Kent, D. V., and Van Couvering, J. A., 1985. The Neogene: Part 2. Neogene geochronology and chronostratigraphy. In Snelling, N. J. (Ed.), *The Chronology of the Geological Record*. Geol. Soc. London Mem., 10:211-260.
- Clement, B. M., and Robinson, F., 1987. The magnetostratigraphy of Leg 94 sediments. In Ruddiman, W. F., Kidd, R. B., Thomas, E., et al., *Init. Repts. DSDP, 94, Pt. 2*: Washington (U.S. Govt. Printing Office), 635-650.
- Emiliani, C., 1955. Pleistocene temperatures. *J. Geol.*, 63:539-578.
- Haq, B. U., Hardenbol, J., and Vail, P. R., 1987. Chronology of fluctuating sea levels since the Triassic. *Science*, 235:1156-1167.
- Haq, B. U., Worsley, T. R., Burckle, L. H., Douglas, R. G., Keigwin, L. D., Opdyke, N. D., Savin, S. M., Sommer, M. A., Vincent, E., and Woodruff, F., 1980. Late Miocene marine carbon-isotopic shift and synchronicity of some phytoplanktonic biostratigraphic events. *Geology*, 8:427-431.
- Hays, J. D., Imbrie, J., and Shackleton, N. J., 1976. Variations in the Earth's orbit: pacemaker of the ice ages. *Science*, 194:1121-1132.
- Hedberg, H. D. (Ed.), 1976. *International Stratigraphic Guide*: New York (Wiley-Interscience).
- Imbrie, J., Hays, J. D., Martinson, D. G., McIntyre, A., Mix, A. C., Morley, J. J., Pisias, N. G., Prell, W. L., and Shackleton, N. J., 1984. The orbital theory of Pleistocene climate: support from a revised chronology of the marine $\delta^{18}\text{O}$ record. In Berger, A., Imbrie, J., Hays, J., Kukla, G., and Saltzman, B. (Eds.), *Milankovitch and Climate* (Pt. 1): Dordrecht (D. Reidel), 269-305.
- Joyce, J. E., Tjalsma, L.R.C., and Prutzman, J. M., 1990. High-resolution planktic stable isotope record and spectral analysis for the last 5.35 m.y.: Ocean Drilling Program Site 625, northeast Gulf of Mexico. *Paleoceanography*, 5:507-529.
- Keigwin, L. D., 1987. Toward a high-resolution chronology for latest Miocene paleoceanographic events. *Paleoceanography*, 2:639-660.
- Keigwin, L. D., Aubry, M.-P., and Kent, D. V., 1987. North Atlantic late Miocene stable-isotope stratigraphy, biostratigraphy, and magnetostratigraphy. In Ruddiman, W. F., Kidd, R. B., Thomas, E., et al., *Init. Repts. DSDP, 94, Pt. 2*: Washington (U.S. Govt. Printing Office), 935-963.
- Kennett, J. P., 1986. Miocene to early Pliocene oxygen and carbon isotope stratigraphy of the Southwest Pacific, DSDP Leg 90. In Kennett, J. P., von der Borch, C. C., et al., *Init. Repts. DSDP, 90*: Washington (U.S. Govt. Printing Office), 1383-1411.
- Killingly, J. S., 1983. Effects of diagenetic recrystallization of $^{18}\text{O}/^{16}\text{O}$ values of deep-sea sediments. *Nature*, 301:594-597.

- Kroopnick, P., 1985. The distribution of ^{13}C of ΣCO_2 in the world oceans. *Deep-Sea Res. Part A*, 32:57–84.
- Miller, K. G., Aubry, M.-P., Khan, K. J., Melillo, A. J., Kent, D. V., and Berggren, W. A., 1985. Oligocene-Miocene biostratigraphy, magnetostratigraphy and isotopic stratigraphy of the western North Atlantic. *Geology*, 13:257–261.
- Miller, K. G., and Curry, W. B., 1982. Eocene to Oligocene benthic foraminiferal isotopic record in the Bay of Biscay. *Nature*, 296:347–350.
- Miller, K. G., and Fairbanks, R. G., 1985. Oligocene to Miocene carbon isotope cycles and abyssal circulation changes. In Sundquist, E. J., and Broecker, W. S. (Eds.), *The Carbon Cycle and Atmospheric CO_2 : Natural Variations Archaean to Present*. Am. Geophys. Union Geophys. Monogr., 32:469–486.
- Miller, K. G., Fairbanks, R. G., and Mountain, G. S., 1987. Tertiary oxygen isotope synthesis, sea-level history, and continental margin erosion. *Paleoceanography*, 2:1–19.
- Miller, K. G., Feigenson, M. D., Wright, J. D., and Clement, B. M., 1991a. Miocene isotope reference section, Deep Sea Drilling Project Site 608: an evaluation of isotope and biostratigraphic resolution. *Paleoceanography*, 6:33–52.
- Miller, K. G., and Kent, D. V., 1987. Testing Cenozoic eustatic changes: the critical role of stratigraphic resolution. *Cushman Found. Foraminiferal Res. Spec. Publ.*, 24:51–56.
- Miller, K. G., Wright, J. D., and Brower, A. N., 1989. Oligocene to Miocene stable isotope stratigraphy and planktonic foraminifer biostratigraphy of the Sierra Leone Rise (DSDP Site 366 and ODP Site 667). In Ruddiman, W., Sarnthein, M., et al., *Proc. ODP, Sci. Results*, 108: College Station, TX (Ocean Drilling Program), 279–294.
- Miller, K. G., Wright, J. D., and Fairbanks, R. G., 1991b. Unlocking the icehouse. *J. Geophys. Res.*, 96:6829–6848.
- North American Commission on Stratigraphic Nomenclature, 1983. North American Stratigraphic Code. *AAPG Bull.*, 67:841–875.
- Pisias, N. G., and Mix, A. C., 1988. Aliasing of the geologic record and the search for long-period Milankovitch cycles. *Paleoceanography*, 3:613–619.
- Pisias, N. G., Shackleton, N. J., and Hall, M. A., 1985. Stable isotope and calcium carbonate records from hydraulic piston cored Hole 574A: high-resolution records from the middle Miocene. In Mayer, L., Theyer, F., Thomas, E., et al., *Init. Repts. DSDP*, 85: Washington (U.S. Govt. Printing Office), 735–748.
- Raymo, M. E., Ruddiman, W. F., Backman, J., Clement, B. M., and Martinson, D. G., 1989. Late Pliocene variation in Northern Hemisphere ice sheets and North Atlantic deep water circulation. *Paleoceanography*, 4:413–446.
- Ruddiman, W. F., Raymo, M., and McIntyre, A., 1986. Matuyama 41,000-year cycles: North Atlantic Ocean and Northern Hemisphere ice sheets. *Earth Planet. Sci. Lett.*, 80:117–129.
- Savin, S. M., Douglas, R. G., and Stehli, F. G., 1975. Tertiary marine paleotemperatures. *Geol. Soc. Am. Bull.*, 86:1499–1510.
- Savin, S. M., Keller, G., Douglas, R. G., Killingley, J. S., Shaughnessy, L., Sommer, M. A., Vincent, E., and Woodruff, F., 1981. Miocene benthic foraminiferal isotope records: a synthesis. *Mar. Micropaleontol.*, 6:423–450.
- Schlich, R., Wise, S. W., Jr., et al., 1989. *Proc. ODP, Init Repts.*, 120: College Station, TX (Ocean Drilling Program).
- Shackleton, N. J., and Kennett, J. P., 1975. Paleotemperature history of the Cenozoic and the initiation of Antarctic glaciation: oxygen and carbon isotope analyses in DSDP Sites 277, 279 and 281. In Kennett, J. P., Houtz, R. E., et al., *Init. Repts. DSDP*, 29: Washington (U.S. Govt. Printing Office), 743–755.
- Shackleton, N. J., and Opdyke, N. D., 1973. Oxygen isotope and palaeomagnetic stratigraphy of equatorial Pacific core V28-238: oxygen isotope temperatures and ice volumes on a 10^5 year and 10^6 year scale. *Quat. Res.*, 3:39–55.
- Vincent, E., and Berger, W. H., 1985. Carbon dioxide and polar cooling in the Miocene: the Monterey Hypothesis. In Sundquist, E., and Broecker, W. S. (Eds.), *The Carbon Cycle and Atmospheric CO_2 : Natural Variations Archaean to Present*. Am. Geophys. Union, Geophys. Monogr. 32:455–468.
- Williams, D. F., Thunell, R. C., Tappa, E., Rio, D., and Raffi, I., 1988. Chronology of the Pleistocene oxygen-isotope record: 0–1.88 m.y.B.P. *Palaeogeogr., Palaeoclimatol., Palaeoecol.*, 64:221–240.
- Woodruff, F., and Savin, S. M., 1989. Miocene deepwater oceanography. *Paleoceanography*, 4:87–140.
- , in press. Mid-Miocene isotope stratigraphy in the deep sea: high-resolution correlations, paleoclimatic cycles, and sediment preservation. *Paleoceanography*.
- Woodruff, F., Savin, S. M., and Douglas, R. G., 1981. Miocene stable isotope record: a detailed deep Pacific Ocean study and its paleoclimatic implications. *Science*, 212:665–668.
- Wright, J. D., Miller, K. G., and Fairbanks, R. G., 1991. Evolution of modern deep-water circulation: evidence from the late Miocene Southern Ocean. *Paleoceanography*, 6:275–290.

Date of initial receipt: 19 January 1990

Date of acceptance: 6 February 1991

Ms 120B-193

APPENDIX

Definition of Bases of Miocene Isotope Zones Mi1a, Mi1b, and Mi7

Zone Mi1a

Type level. Hole 563, Sample 82-563-14-2, 129–135 cm (282.79 mbsf)

Age estimate. 21.8 Ma

Correlation.

First order: Chronozone C6Ar; near the top of N4b; LO of *Globorotalia kugleri* in Section 82-563-14-1; Miller et al. (1985)

Second order: NN2

Locations observed. Benthic $\delta^{18}\text{O}$ records: Sites 563 (Miller and Fairbanks, 1985; Wright, unpubl. data), Sites 366 and 667 (Miller et al., 1989), and Site 704 (Wright, unpubl. data)

Zone Mi1b

Type level. Hole 608, Sample 94-608H-38H-1, 66–70 cm (349.16 mbsf)

Age estimate. 18.1 Ma

Correlation.

First order: Chronozone C6Dr

Second order: Planktonic foraminifer Zone N6

Locations observed. Benthic $\delta^{18}\text{O}$ records: Sites 563 (Miller and Fairbanks, 1985; Wright, unpubl. data), Sites 366 and 667 (Miller et al., 1989), Site 704 (Wright, unpubl. data), and Site 588 (Kennett, 1986)

Zone Mi7*

Type level. Hole 608, Sample 94-608H-22-4, 80–84 cm (200.20 mbsf)

Age estimate. 8.5 Ma

Correlation.

First order: Chronozone C4Ar

Second order: Planktonic foraminifer Zone N16

Locations observed. Benthic $\delta^{18}\text{O}$ records: Sites 563 (Miller and Fairbanks, 1985; Wright, unpubl. data), Site 704 (Wright and Miller, unpubl. data), and Site 289 (Woodruff et al., 1981; Savin et al., 1981)

*Zone Mi7 is not formally recognized as an isotope zonation, but it is useful for upper Miocene correlations.

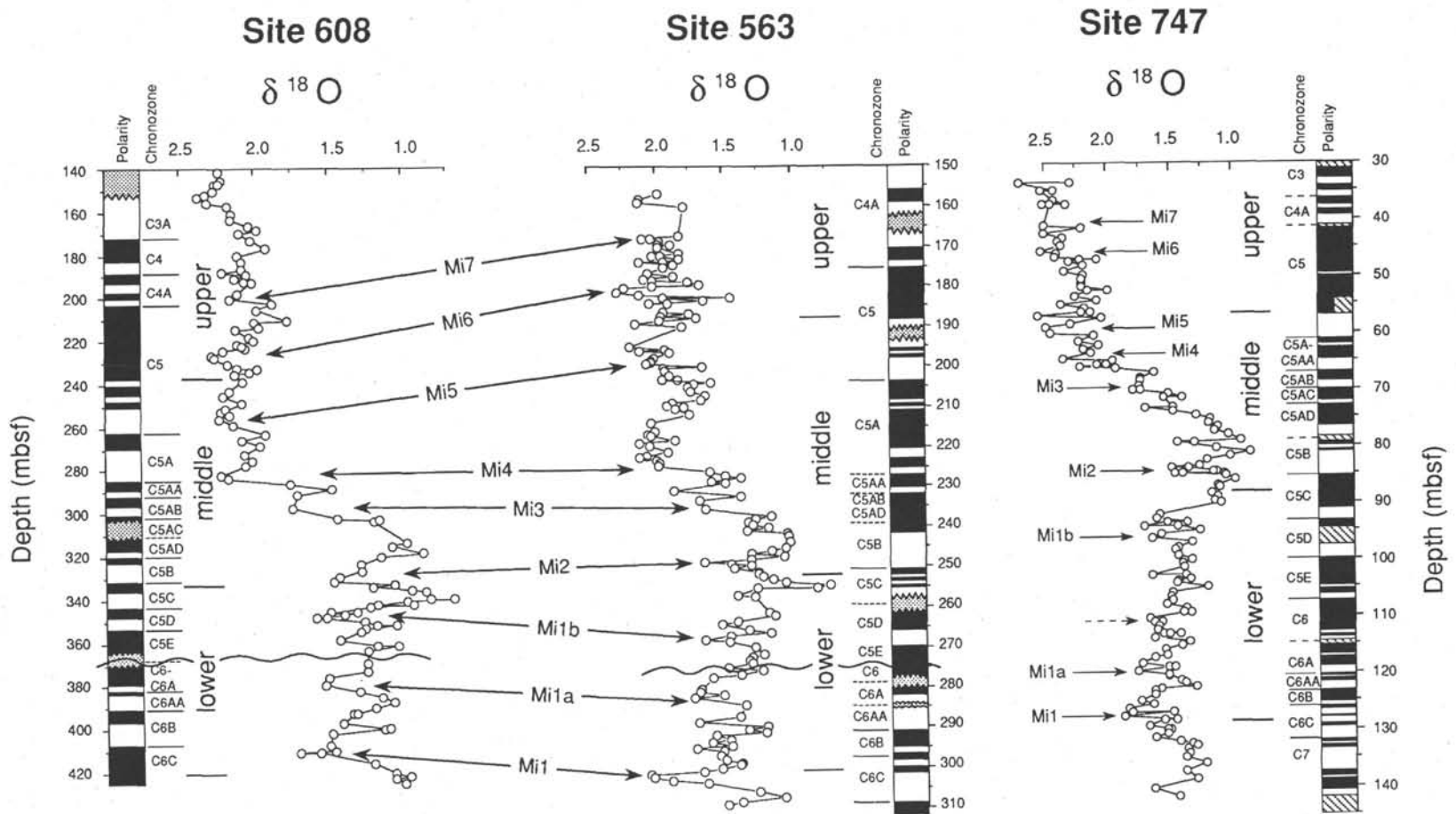


Figure 5. Oxygen isotope events identified at DSDP Sites 563 and 608. Correlative levels at Site 747 are indicated by arrows. Chronozones Mi1 and Mi2-Mi6 are defined by Miller et al. (in press), whereas Chronozones Mi1a, Mi1b, and Mi7 are discussed in this study.

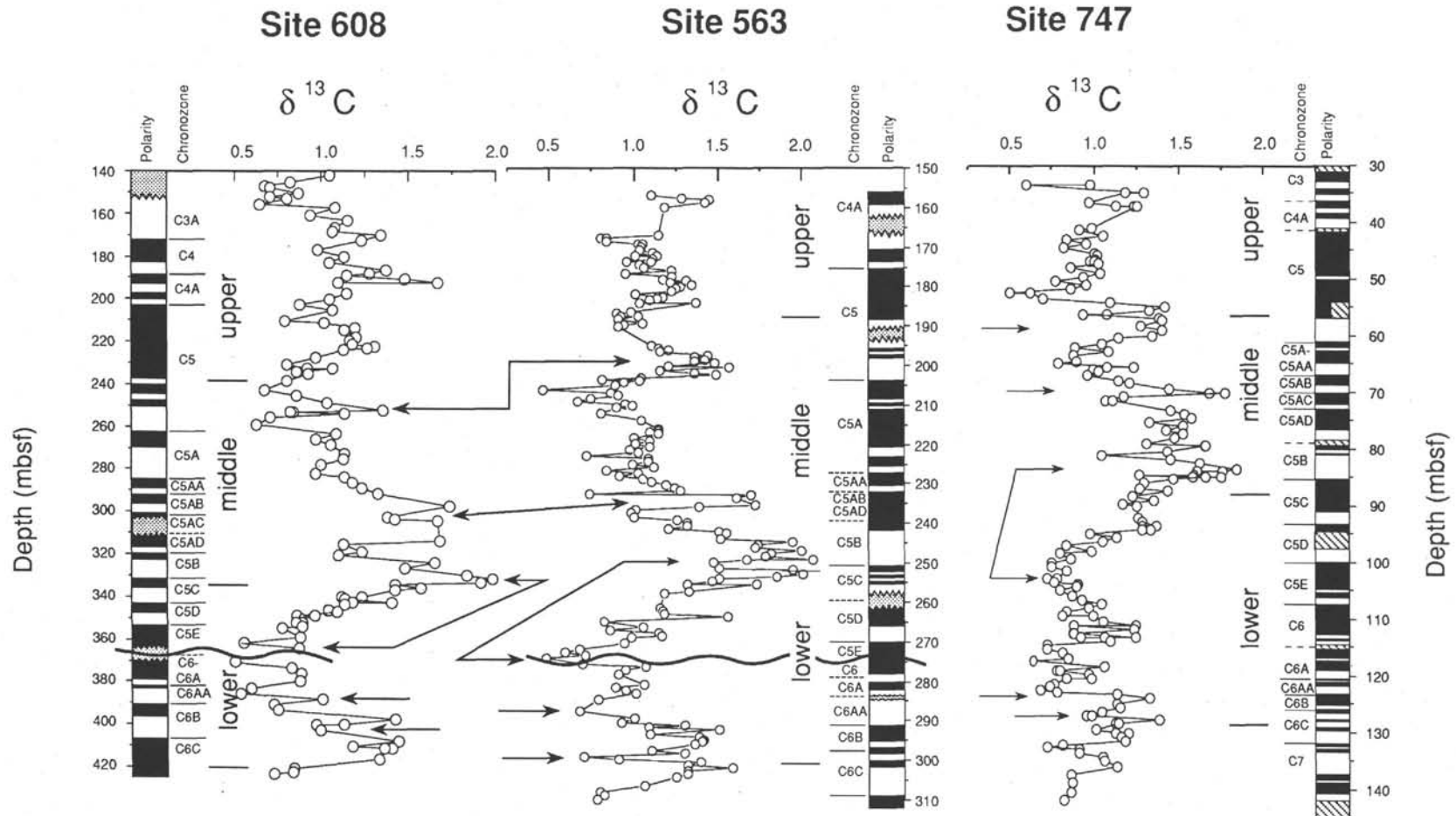


Figure 6. Carbon isotope events identified at DSDP Sites 563 and 608. Correlative levels at ODP Site 747 are also indicated. The lower Miocene $\delta^{13}\text{C}$ increase is represented by an interval at both Sites 563 and 608. The interval from 109 to 103 mbsf at Site 747 represents a zone of uncertain correlation (see text).